Am J Cancer Res 2023;13(6):2598-2616
www.ajcr.us /ISSN:2156-6976/ajcr0150572

Original Article

Therapeutic potential of EGFR/mTOR/Nf-kb targeting small molecule for the treatment of non-small cell lung cancer

Bashir Lawal[1,2*], Yu-Cheng Kuo[3,4*], Alexander TH Wu[5,6,7,8], Hsu-Shan Huang[8,9,10,11,12]

[1]UPMC Hillman Cancer Center, University of Pittsburgh, Pittsburgh, PA 15260, USA; [2]Department of Pathology, University of Pittsburgh, Pittsburgh, PA 15260, USA; [3]Department of Pharmacology, School of Medicine, College of Medicine, Taipei Medical University, Taipei 11031, Taiwan; [4]School of Post-baccalaureate Chinese Medicine, College of Chinese Medicine, China Medical University, Taichung 40402, Taiwan; [5]The PhD Program of Translational Medicine, College of Medical Science and Technology, Taipei Medical University, Taipei 11031, Taiwan; [6]Clinical Research Center, Taipei Medical University Hospital, Taipei Medical University, Taipei 11031, Taiwan; [7]TMU Research Center of Cancer Translational Medicine, Taipei Medical University, Taipei 11031, Taiwan; [8]Graduate Institute of Medical Sciences, National Defense Medical Center, Taipei 11490, Taiwan; [9]PhD Program for Cancer Molecular Biology and Drug Discovery, College of Medical Science and Technology, Taipei Medical University and Academia Sinica, Taipei 11031, Taiwan; [10]Graduate Institute for Cancer Biology and Drug Discovery, College of Medical Science and Technology, Taipei Medical University, Taipei 11031, Taiwan; [11]School of Pharmacy, National Defense Medical Center, Taipei 11490, Taiwan; [12]PhD Program in Drug Discovery and Development Industry, College of Pharmacy, Taipei Medical University, Taipei 11031, Taiwan. [*]Equal contributors.

Received April 5, 2023; Accepted May 28, 2023; Epub June 15, 2023; Published June 30, 2023

Abstract: Despite the therapeutic advancement with chemotherapy and targeted therapy against non-small-cell lung cancer (NSCLC), most patients ultimately develop resistance to these drugs, exhibiting disease progression, metastasis, and worse prognosis. There is, therefore, a need for the development of novel multi-targeted therapies that can offer a high therapeutic index with lesser chances of drug resistance against NSCLC. In the present study, we evaluated the therapeutic potential of a novel multi-target small molecule NLOC-015A for targeted treatment of NSCLC. Our in vitro studies revealed that NLOC-015A exhibited a broad spectrum of anticancer activities against lung cancer cell line. NLOC-015A decreased the viability of H1975 and H1299 cells with respective IC_{50} values of 2.07±0.19 and 1.90±0.23 μm. In addition, NLOC-015A attenuated the oncogenic properties (colony formation, migratory ability, and spheroid formation) with concomitant downregulation of expression levels of epidermal growth factor receptor (EGFR)/mammalian target of rapamycin (mTOR)/AKT, nuclear factor (NF)-κB, signaling network. In addition, the stemness inhibitory effect of NLOC0-15A was accompanied by decreased expression levels of aldehyde dehydrogenase (ALDH), MYC Proto-Oncogene (C-Myc), and (sex-determining region Y)-box 2 (SOX2) in both H1975 and H1299 cell lines. Furthermore, NLOC-015A suppressed the tumor burden and increased the body weight and survival of H1975 xenograft-bearing mice. Treatment with NLOC-015A also attenuated biochemical and hematological alterations in the tumor bearing mice. Interestingly, NLOC-015A synergistically enhanced the *in vitro* efficacy, and therapeutic outcome of osimertinib *in vivo*. In addition, the toxicity of osimertinib was significantly attenuated by combination with NLOC-015A. Altogether, our findings suggested that combining osimertinib with NLOC-015 appears to be a promising way to improve osimertinib's efficacy and achieve better therapeutic results against NSCLC. We therefore suggest that NLOC-015A might represent a new candidate for treating NSCLC via acting as a multitarget inhibitor of EGFR/mTOR/NF-Kb signaling networks and efficiently compromising the oncogenic phenotype of NSCLC.

Keywords: NLOC-15A, small molecule, non-small-cell lung cancer (NSCLC), epidermal growth factor receptor (EGFR)

Introduction

According to the latest WHO reports, lung cancer is the second most commonly diagnosed cancer [1, 2], and causes the highest death compared to other cancers worldwide [1]. In 2020, lung cancer accounts for about 12% to 13% of new cases, and about 22% to 23% of

cancer death in males and females, respectively [3]. The five-year survival rate of patients has been reported as low < 15% [4], reflecting a lack of effective long-term treatment. Lung cancer has been classified as small-cell lung cancer (SCLC) and Non-small-cell lung cancer (NSCLC). However, NSCLC contributes about 85% of all lung cancers [5] including adenocarcinomas and squamous cell carcinomas [6]. An extensive number of risk factors including environmental pollution, smoking, irradiation, genetic alterations, etc. have been attributed to the increased prevalence and progression of lung cancer [7].

Accumulating evidence from clinical and genome sequencing studies have shown that drivers, such as Kirsten rat sarcoma viral oncogene (KRAS) [8], epidermal growth factor receptor (EGFR) mutation [9], mesenchymal-epithelial transition (MET) amplification [10], and human epidermal growth factor receptor 2 (HER2), mutations are greatly linked with increased risk of lung cancer development, metastasis and drug resistance via modulation of downstream signaling network. Among these driver genes, EGFR is the most widely mutated and implicated in lung cancer angiogenesis, cell proliferation, apoptosis inhibition, metastasis, and drug sensitivity and resistance [11]. EGFR exert its oncogenic role via regulation of the phosphatidylinositol 3-kinase (PI3K)/AKT, Janus kinase 2 (JAK2)/signal transducer and activator of transcription 3 (STAT3), and Ras/mitogen-activated protein kinase (MAPK) pathways [12-14]. Consequently, three generations of EGFR-tyrosine kinase inhibitors (TKIs), for target therapy against EGFR driven NSCLC have been developed with significant clinical success against EGFR-driven NSCLC [15]. Despite these advances, further improvements are needed as the majority of patients ultimately develop resistance to the first, second and third generation of TKIs [16], exhibiting disease progression, metastasis and worse prognosis [3, 16]. There is, therefore, a need for the development of novel targeted therapies that can offer a high therapeutic index against NSCLC with lesser chances of drug resistance and adverse effect when compared to chemotherapy. However, to the best of our knowledge, no previous studies identified a molecule that can connectively modulate the EGFR, and PI3K-TOR pathways in NSCLC.

Due to the higher efficacy and safety compared with traditional chemotherapy drugs, multi-targeted small drugs for the treatment of human cancers have transformed the concept of oncological medicine [17, 18]. Our in-house synthesized multi-target small molecules have received great therapeutic success with translational relevance for the treatment of cancers, inflammations, and immune-related disorders [19-39].

Biphenyl, and isoflavones are natural product backbones with a vast range of biological activities [40, 41]. Difluorophenyl is an important bioactive substituent group that has been implicated in the biological activities of several drugs [42]. Niclosamide is a multipurpose compound with proven efficacy in treating several diseases, including cancers [43, 44]. Consequently, in the present study, we employ a structurally guided pharmacophore hybridization and scaffold-hopping [45] of these bioactive scaffolds to design and synthesis a novel small molecules, NLOC-015A. Subsequently, we demonstrated that NLOC-015A suppresses the proliferation and oncogenic phenotypes of NSCLC via inhibiting the EGFR/mTOR, signaling network. Furthermore, NLOC-015A synergistically enhanced the anti-NSCLC activities of osimertinib and attenuated disease-induced alterations of biochemical and hematological parameters in NSCLC bearing tumor xenograft mice. We, therefore, suggest that NLOC-015A might represent a new candidate for treating NSCLC.

Materials and methods

Cell lines and culture

A total of 60 human tumor cancer cell lines from nine different tissue origins; breast, colon, brain, kidneys, hemopoietic cells, lungs, prostate, ovaries, and melanocytes were obtained from the US-National Cancer Institute-Developmental Therapeutics Program (DTP). In addition, two other NSCLC cell lines (H1299 and H1975) obtained from American Type Culture Collection (ATCC, Manassas, VA, USA) were cultured/subcultured at 90%~95% confluence in Roswell Park Memorial Institute (RPMI) 1640 medium supplemented with 10% fetal bovine serum (FBS) (Gibco) and 1% penicillin/streptomycin (Invitrogen, Life Technolo-

gies, Carlsbad, CA, USA) under standard incubator condition (37°C in 5% humidified CO_2).

Synthesis of NL0C-015A

The starting material of diflunisal (2',4'-difluoro-4-hydroxy-[1,1'-biphenyl]-3-carboxylic acid) was synthesized via a previously described stepwise protocol [30]. Four millimolar (0.98) of diflunisal was prepared in anhydrous tetrahydrofuran (30 mL), mixed with 1 mL of thionyl chloride (14 mmol), and refluxed under a nitrogen atmosphere for 8 h. The resulting mixture was cooled to 27°C, steamed, and reacted with an anhydrous tetrahydrofuran solution of 3,4-difluoroaniline (0.4 mL, 4 mmol) for 14 h. Subsequently the reaction mixture was washed with ethyl acetate/n-hexane and extracted with ethyl acetate followed by stepwise washing with 10% $NaHCO_3$ (15 mL), double-distilled (dd) H_2O, and brine (10 mL), and dried over anhydrous $MgSO_4$ to obtain a white intermediate compound, (N-(3,4-difluorophenyl)-2',4'-difluoro-4-hydroxy-[1,1'-biphenyl]-3-carboxamide) [30], which was further cyclized to NL0C-015A (6-(2,4-difluorophenyl)-3-(3,4-difluorophenyl)-2H-benzo[e][1,3] oxazine-2,4(3H)-dione) in the presence of methyl chloroformate and pyridine [31].

Cell-viability assay

A cell-viability assay was conducted using the sulforhodamine B (SRB; Sigma-Aldrich, Taipei, Taiwan) reagent as described previously [46]. Cells were harvested at 80% confluence and seeded in 96-well plates (10^4 cells/well) for 24 h followed by treatment with graded concentrations of NL0C-015A (0-3.2 1 μm), osimertinib, or a combination of the two drugs. After 48 h of drug treatment, cells were fixed with trichloroacetic acid (TCA; 10%) for 1 h and then stained with 0.4% (w/v) SRB. Unbound SRB was washed out with 1% (v/v) acetic acid and allowed to dry overnight. The contents of the plate were further solubilized in 20 mM Tris-buffer, and the absorbance was recorded at 562 nm with the aid of a microplate reader (Molecular Devices, Sunnyvale, CA, USA). Possible synergetic/antagonistic effects of NL0C-015A and osimertinib were evaluated by analyzing the combination index (CI) using CompuSyn software for Drug Combinations [47]. Accordingly, CI values of < 1 were considered to be synergism, = 1 indicated an additive effect, and > 1 represented an antagonistic effect of the two drugs [48].

Cell-migration assay

NSCLC cells (H1299 and H1975) were seeded into two-well (10^5 cells in 100 μL media/well) silicon inserts placed in six-well plates and incubated for 24 h. After incubation, the medium was siphoned off, and the insert was carefully removed, followed by the addition of fresh medium containing NL0C-015A (1 μm). A wound scratch was made on the plate. The wound was photographed under a microscope (Olympus CKX53 Cell Culture microscope) immediately after treatment (0 h) and after 24 h, and wound closure was quantified with the aid of NIH ImageJ software (https://imagej.nih.gov/ij/).

Colony-formation assay

A method modified from Franken et al. [49] was used to assess the effect of NL0C-015A treatments on colony formation by H1299 and H1975 cells. Briefly, 300 cells were seeded in six-well plates and treated with NL0C-015A (1 μm). Cells were allowed to grow for a week, and the colony-formation inhibitory effect of the drug was assessed relative to untreated cells using an SRB fixation protocol.

Tumor sphere formation assay

The sphere formation assay was conducted according to the method described by Ma et al. [50]. Briefly, the NSCLC cells (H1299 and H1975) were seeded into the ultra-low-attachment six-well plates (5×10^3 cells per well) containing stem cell medium; serum-free RPMI 1640 medium supplemented with B27 and 20 ng/mL human basic fibroblast growth factor (bFGF) (Invitrogen, Grand Island, NY, USA), and epidermal growth factor (20 ng/mL, Millipore, Bedford, MA). The plates were incubated in the presence (NL0C-015A, 1 μm), or absence of drug treatment. The medium was changed every 72 h. After 7 days of incubation, the aggregated spheres (diameter > 50 μm) were counted and photographed with an inverted phase-contrast microscope.

Western blot analysis

After 48 hrs of drug treatment, the total protein lysates from NL0C-015A-treated and untreated

cells were harvested using a protein lysis buffer (containing proteinase inhibitors and phosphatase inhibitors, RIPA). Protein lysates (25 μg) were denatured and separated using a 10% sodium dodecylsulfate polyacrylamide gel electrophoresis (SDS-PAGE) gel [51]. Proteins were transferred onto nitrocellulose membranes and blocked in 5% skim milk followed by washing with TBST (0.2% Tween-20, 50 mM Tris-HCl at pH 7.5, and 150 mM NaCl). Following overnight incubation (at -4°C) with respective primary antibodies against mTOR (diluted 1:1000, cat. no.: 2983, Cell Signaling Technology, Danvers, MA, USA), Akt (diluted 1:1000, cat. no.: 4691, Cell Signaling Technology), NF-κB (diluted 1:1000, cat. no.: 8242, Cell Signaling Technology). The membrane was incubated with appropriate horseradish peroxidase-conjugated secondary antibodies for 60 min. Protein-antibody interactions were detected with an enhanced chemiluminescence (ECL) kit (ECL-Plus, Amersham Pharmacia Biotech, Piscataway, NJ, USA), and the band image was captured using the BioSpectrum® Imaging System (Upland, CA, USA). GAPDH was used as an internal control to confirm equal gel loading.

In vivo studies

Animal experiments were approved by and conducted in strict compliance with the ethical conduct of Taipei Medical University as contained in the Affidavit of Approval (approval no. LAC-2017-0161). In total, 24 female NOD/SCID mice (6 weeks old with an average weight of 25.32±1.24 g) were obtained from BioLASCO (Taipei, Taiwan) and maintained under standard lab conditions at the Animal Center of Taipei Medical University. Mice were randomly divided into four groups (n = 6), and 5 × 10^5 H1975 cells were subcutaneously injected into the right hind flank, and tumors were allowed to grow. Mice in groups A~C were respectively treated with NLOC-015A only (5 mg/kg body weight (BW) five times/week), osimertinib only (5 mg/kg BW five times/week), and combined treatment (5 mg/kg BW five times/week), while group D mice served as the control and received 0.5 mL PBS. BW changes and tumor growth were monitored on a weekly basis using an electronic weighing balance and standard calipers. The final tumor volume was computed using the formula: tumor volume = ½ (length × width^2) [52, 53]. After 4 weeks of treatment, animals were placed on mild ether anesthesia and humanly sacrificed as described previously [54, 55], after which blood samples were collected into free-tubes and EDTA-containing tubes and were respectively processed for subsequent biochemical and hematological analyses. Following blood sample collection, the animals were quickly dissected, and the tumors, liver, kidneys, and lungs were carefully harvested and processed for further analyses.

Analysis of hematological and biochemical parameters

Blood samples from treated and control mice were analyzed for levels of hematological components including hemoglobin (HGB), hematocrit (HCT), red blood cells (RBC) counts, white blood cell (WBC) counts, mean corpuscular hemoglobin (MCH), mean corpuscular volume (MCV), and mean corpuscular hemoglobin concentration (MCHC) using an automated hematologic analyzer (Sysmex, KX-21, Japan) as described by Dacie and Lewis [56]. All biochemical analyses including serum activities of alanine transaminase (ALT) and aspartate transaminase (AST), and concentrations of serum electrolytes (Na, K, and Cl), total protein, bilirubin, albumin, urea, and creatinine were analyzed using an automated chemical analyzer according to established protocols [57-63].

Statistical analysis

Replicates of the experimental data were analyzed using GraphPad Prism vers. 6.04 for Windows (GraphPad Software, La Jolla, CA, USA). Results were computed as the mean ± SD of the replicates. One-way analysis of variance (ANOVA), followed by Duncan post hoc test was performed for statistical comparison within the groups. Data from treatment groups were compared with the control using Student's *t*-test. Data were considered statistically significance at $P < 0.05$ (*), $P < 0.001$ (**), and $P < 0.0001$ (***).

Results

Rationale for structurally guided pharmacophore hybridization strategy for the design and synthesis of NLOC-series of compounds

Pharmacophore hybridization and scaffold-hopping of bioactive compounds are important

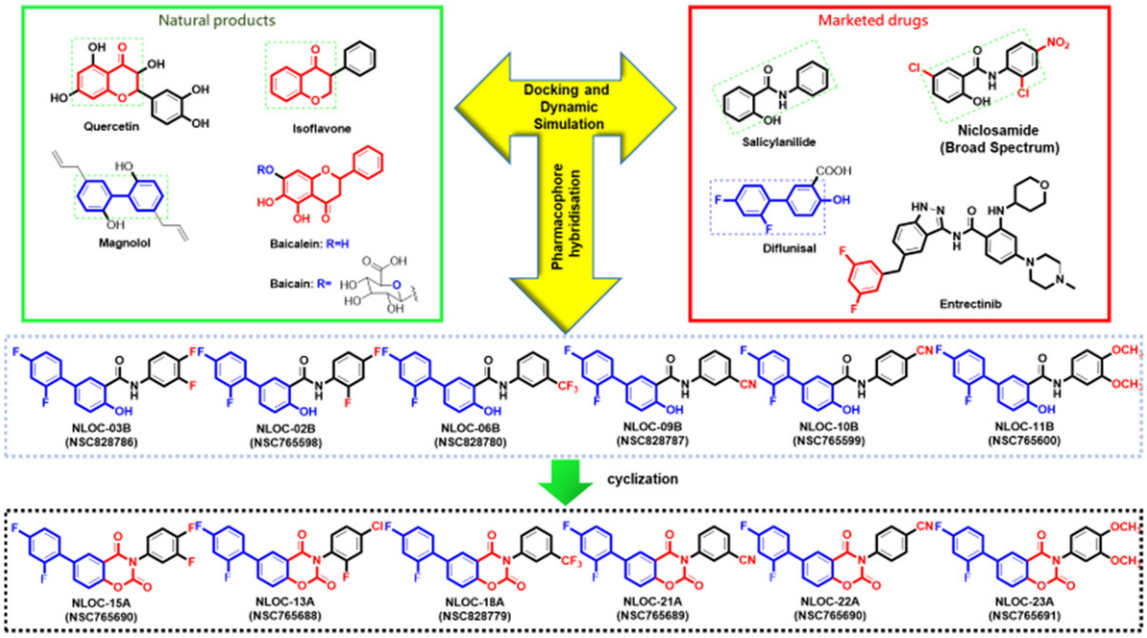

Figure 1. Schematic illustration of the proposed drug design strategy and the current work. Structurally guided pharmacophore hybridization strategy for the design and development of a series of NLOC compounds.

approach for novel drug design and development [45]. Biphenyl, and isoflavones are important natural product backbones, and several bioactive compounds containing these backbones were reported to have a vast range of biological activities, including antioxidative, anti-atherosclerosis, muscle relaxant, antimicrobial, anti-inflammatory, and anticancer effects [40, 41]. A difluorophenyl is an important bioactive compound that has been implicated in the biological activities of several drugs. A number of clinical drugs, e.g., diflunisal contain difluorophenyl as the major bioactive moieties responsible for its pharmacological activities (anticancer, anti-arthritis, analgesic, and anti-inflammatory properties) [42]. In addition, entrectinib contains difluorophenyl as the major anticancer component responsible for its bioactivity. Niclosamide is a multipurpose clinical small molecule with several biological activities including antihelmintic, antioxidant, antimicrobial, anti-inflammatory, anticancer and immune-modulatory properties [43, 44]. Therefore, due to the various activities mentioned above, these compounds and their derivatives may represent target compounds worthy of preclinical evaluation and future clinical trials for the treatment of cancer. In the present study, the structurally guided pharmacophore hybridisation strategy of these bioactive scaffolds (flavones and isoflavones), biphenyl, difluorophenyl, and salicylanilide led to the discovery and synthesis of following structurally related novel small molecules (**Figure 1**).

In silico structural-activity based profiling strongly suggest the potential of NLOC-015A for the treatment of lung cancer and associated inflammatory condition

Following the design and synthesis, and prior to our experimental validations, we used the PASS (prediction of activity spectra for substances) algorithm to evaluate the potential applications of NLOC-015A based on the in silico structural-activity relationship. Interestingly, our structural-activity related profiling revealed that NLOC-015A could be useful as antineoplastic, anti-inflammatory, for the treatment of biliary tract, hepatic, renal and prostate disorders. In addition, the compound could be used as an inhibitor of cyclooxygenase, MAP2K, EGF, STAT, and P13K (Table S1). Specific anti-cancer profiling against common cancer cell lines revealed the high anti-proliferative potential of NLOC-015A against the lung cancer cell lines including A549, and NCI-H128; Colon cancer cell lines including RKO, and HCT-116; and pancreatic cancer lines including HuP-T3 and CFPAC-1 (Table S2). Collectively, our in silico structural-activity based profiling strongly suggests the potential of NLOC-015A for the treatment of

lung cancer and associated inflammatory condition.

Screening and selection of first-in class compound with higher efficacy against lung cancer

We explored the availability of well-characterized US National Cancer Institute (NCI)-60 human tumor cell lines to screen the anticancer profile of the 12 compounds against multiple cell line panels of human cancers from nine different tissue origins; breast, colon, brain, kidneys, hemopoietic cells, lungs, prostate, ovaries, and melanocytes through the Development Therapeutics Program (DTP) of the NCI [64, 65]. The compounds were first evaluated for anti-proliferative and cytotoxic effects at an initial single dose of 10 μM. Compounds demonstrating satisfactory anticancer profile at single dose treatment, were subsequently selected, and screened for dose-dependent responses. Among the 12 compounds, we found that only NLOC-011 and NLOC23 demonstrated no significant anticancer activities against the NCI-60 cell lines and thus were not selected for subsequent analysis. However, the remaining 10 compounds including the NLOC-02, NLOC-03, NLOC-06, NLOC-09, NLOC-10, NLOC-15, NLOC-018, NLOC-21, and NLOC-22 demonstrated significant anticancer activities and were thus evaluated for dose-dependent activities against nine cell lines subsets of human non-small cell lung cancer (**Figure 2**), revealing dose dependent antiproliferative activities with IC_{50} ranging 0.96±0.24 to 2.77±0.34 μM (**Table 1**). Among the 3 compounds (NLOC-15, NLOC-21, and NLOC-22) that demonstrated the highest activities (lowest mean IC_{50}), only NLOC-015A exhibited activities against all the nine cell lines of NSCLC (**Table 1**). In addition, this compound also demonstrated significant anti-cancer activities against other human tumor cell line origins (**Figure 3A** and **3B**). Hence, this compound was selected for subsequent functional mechanistic analysis against 2 NSCLC cell lines: H1299 and H1975.

NCI-DTP COMPARE analysis revealed that NLOC-015A shared similar antitumor fingerprint with NCI-mechanistic mechanistic of EGFR/PI3K/AKT/mTOR signaling network

The US-National Cancer Institute-Developmental Therapeutics Program (DTP)-COMPARE analysis revealed high anti-cancer fingerprint similarities with several synthetic compounds including Niclosamide, Dibromsalan, three members of NLOC series (NLOC-10B, NLOC-21A, and NLOC-2B) and other compounds with high fingerprint correlation (cor; 0.55~0.92), and common cell line counts (CCLCs; 47~57). Except for 4-chloro-2,6-bis [5-chloro-3-(chloromethyl)-2-hydroxyphenyl]-methyl] phenol (MW; 506.6 g/mol), all other NCI-synthetic compounds presented to shares similar antitumor fingerprints with NLOC-015A are small molecules (MW; 297.7~445.8 g/mol). The identity, cor-value, common cell counts, and molecular weight of the synthetic compounds are also shown in **Table 2**. Interestingly, the NCI- investigational and mechanistic drugs with highly similar (cor; 0.34~0.75) anticancer fingerprint of NLOC-15A included several mechanistic inhibitors of EGFR/ PI3K/Akt/mTOR/MET signaling pathways. Subsequently, we explored the potential of NLOC-015A as a therapeutic target against this signature.

NL0C-015A compromised the cell viability and oncogenic phenotypes of NSCLC via inhibition of the EGFR//mTOR/NF-Kb signaling pathways, and synergistically enhanced the antitumorigenic activities of osimertinib in NSCLC cells

We evaluated the effects of NL0C-015A on the viability and oncogenic phenotypes of NSCLC cells. Our results revealed that treatments with NL0C-015A progressively decreased the viability of H1975 and H1299 cells with respective IC_{50} values of 2.07±0.19 and 1.90±0.23 μm (**Figure 4A**). Furthermore, treatment with NL0C-015A significantly inhibited the colony-formation (**Figure 4B**) and migratory abilities (**Figure 4C**) of H1299 and H1975 cells. A Western blot analysis indicated that NL0C-015A significantly decreased expression levels mTOR, AKT, p-AKT, NF-κB, and EGFR, in both the H1975 and H1299 cell lines (**Figure 4D**). Collectively, our results demonstrated that NL0C-015A compromised the oncogenic phenotypes of NSCLC cells via modulation of the EGFR- and PI3K-TOR signaling pathways.

Combination therapy is seen as one of the strategies for improving drug efficacy and ameliorating drug resistance associated with single therapies. Therefore, we assessed the possible effect of NL0C-015A in combination with

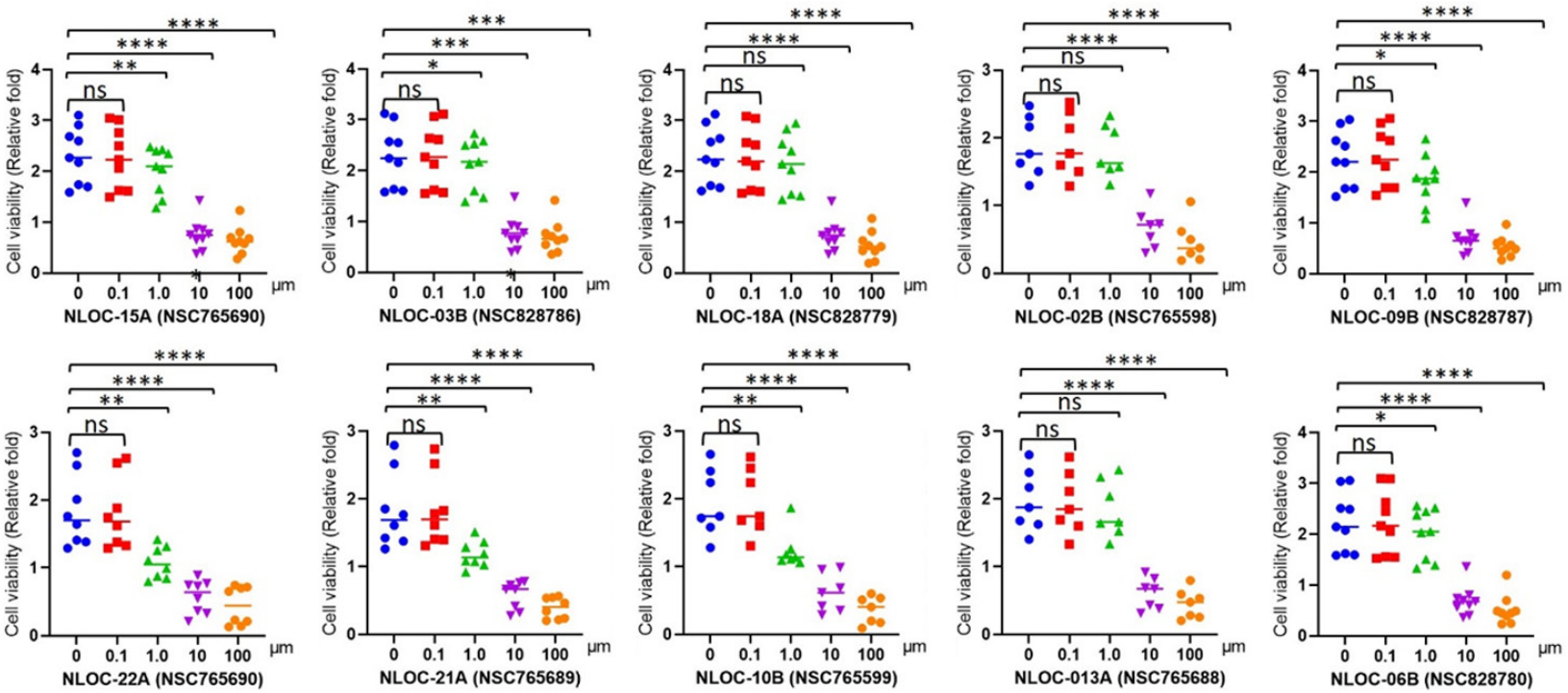

Figure 2. In vitro anti-proliferative effect of the 12 structurally related small molecule derivatives of niclosamide against the 9 cell lines subsets of human non-small cell lung cancer. The cell line used include; A549/ATCC, EKVX, HOP-62, HOP-92, NCI-H226, NCI-H23, NCI-H322M, NCI-H460, and NCI-H522. *P < 0.05, **P < 0.01, ***P < 0.001, ****P < 0.0001.

Table 1. The half maximal inhibitory concentrations (IC_{50}) of structurally related small molecule derivatives of niclosamide against the 9 cell lines subsets of human non-small cell lung cancer

Compounds	IC_{50} (half maximal inhibitory concentration; (μM))									
	A549/ATCC	EKVX	HOP-62	HOP-92	NCI-H226	NCI-H23	NCI-H322M	NCI-H460	NCI-H522	MEAN ± SD
NLOC-02	2.640	-	3.950	1.120	3.530	2.390	2.780	3.040	-	2.77±0.34
NLOC-03	1.570	1.380	1.590	0.684	1.510	1.070	1.560	1.460	0.923	1.30±0.11
NLOC-06	3.260	2.280	2.930	0.824	2.010	1.890	2.760	2.670	1.320	2.21±0.26
NLOC-09	3.520	2.680	2.390	0.338	1.860	1.490	2.230	1.420	0.642	1.84±0.33
NLOC-10	1.050	-	2.510	0.219	1.730	0.395	1.300	0.569	-	1.11±0.30
NLOC-13	2.550	-	3.110	0.920	2.530	2.090	2.370	2.940	-	2.35±0.27
NLOC-15	1.580	1.460	1.410	0.389	1.410	0.936	1.450	1.320	0.666	1.18±0.13
NLOC-18	1.680	1.180	1.480	0.952	1.510	1.130	1.340	1.530	1.420	1.35±0.07
NLOC-21	1.870	-	1.880	0.239	0.554	0.406	1.810	0.850	0.357	0.995±0.25
NLOC-22	1.875	-	1.900	0.239	1.300	0.331	1.260	0.556	0.281	0.96±0.24

-: No activity.

osimertinib. Interestingly synergetic CI indices in the ranges of 0.27~0.95 and 0.33~0.96 were respectively obtained for H1975 and H1299 cells (**Figure 4E**), thus indicating that NLOC-015A and osimertinib acted synergistically to suppress the viability of NSCLC cells.

NLOC-015A inhibited the spheroid-forming ability NSCLC via inhibition ALDH/C-MYC/SOX2

Our further analysis revealed that the spheroid-forming abilities of H1975 and H1299 cells were compromised by NLOC-015A treatment (**Figure 5A**). Western blot analysis revealed that H1975 and H1299 spheroid exhibited higher expression levels of ALDH, C-MYC and SOX2 when compared with their respective parental cell line controls (**Figure 5B**). Collectively, our results demonstrated that NLOC-015A inhibited the spheroid-forming ability NSCLC via inhibition ALDH/C-MYC/SOX2.

NLOC-015A suppressed tumorigenesis and enhanced the in vivo efficacy of osimertinib in a xenograft model of NSCLC

We explored a mouse xenograft model to evaluate the *in vivo* anticancer activities of NLOC-015A alone and in combination with osimertinib (**Figure 6A**). NLOC-015A alone significantly suppressed H1975 tumor growth (**Figure 6A**, **6B**), enhanced the survival (**Figure 6C**) and weight gain (**Figure 6D**) of animals despite the decrease feed intake (**Figure 6E**) compared to the vehicle control. Interestingly, treatment with a combination of NLOC-015A and osimertinib achieved significantly higher *in vivo* efficacy compared to individual therapy. These findings suggested that NLOC-015A synergized with osimertinib to elicit higher antitumorigenic activities in NSCLC.

NLOC-015A attenuated biochemical and hematological alterations in NSCLC tumor bearing mice

We evaluated the effect of NLOC-015A treatment on hematological and serum biochemical parameters of the liver and kidney integrity in NSCLC tumor-bearing mice (**Figure 7**; **Table 3**). Our analysis revealed the elevated levels of serum transaminases (serum glutamic-oxaloacetic transaminase (SGOT) and serum glutamic pyruvic transaminase (SGPT)), total proteins, and uric acid (UA) in NSCLC tumor-bearing mice. These alterations were significantly attenuated by combined treatment compared to the individual treatment (**Table 3**). Furthermore, combined therapy attenuated elevated levels of potassium and creatinine that were observed in the serum of osimertinib-treated mice. An analysis of hematological parameters found that no tumor or treatment-mediated changes were observed in erythrocytic indices (RBCs, HGB, HCT, MCV, MCHC, MCH, or RDW-cv). However, leukocytosis, characterized by elevated WBCs, neutrophils (NEUTs), monocytes (MONOs), and eosinophils (EOSs), was observed in osimertinib-treated mice. However, combined treatment with osimertinib and NLOC-015A significantly ameliorated the elevated leucocytic indices. Similarly, thrombocytosis, marked by elevated platelets (PLTs) and decreased P-LCR counts observed in control

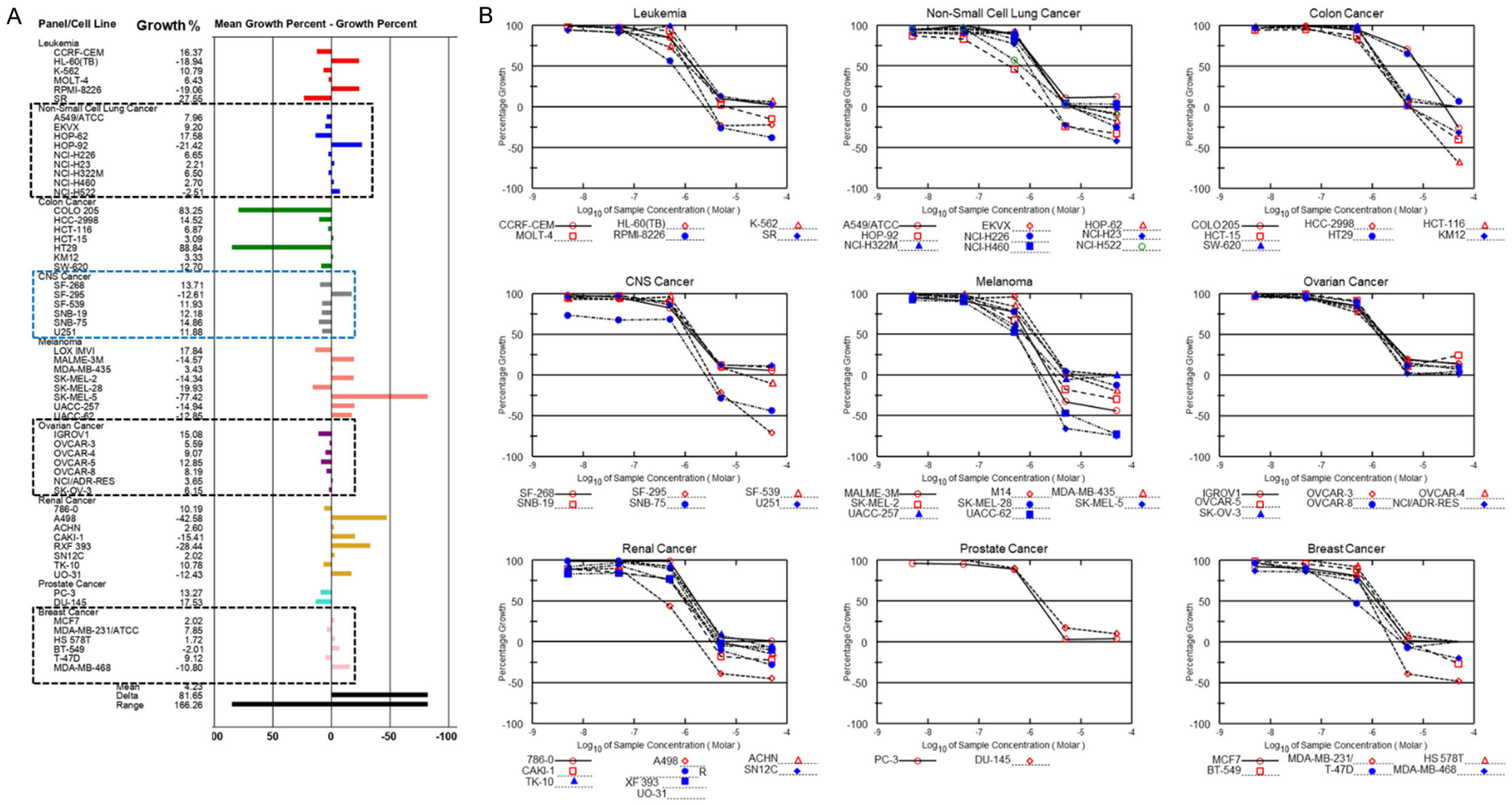

Figure 3. High throughput in vitro anti-cancer screening of NLOC-015A against the 60-cancer-cell-line of the US-National Cancer Institute-Developmental Therapeutics Program (DTP). A. Anti-proliferative effect of NLOC-015A against panels of 60 human cancer cell lines. Each cell line was treated with a single dose of (10 μM) of NLOC-015A. The zero points represents the mean percentage of cell growth. The percentage growth inhibition of each cell line relative to the mean is represented by values under 100 (antiproliferative), whereas those values below 0 indicate cell death (cytotoxic effect). B. Dose-cytotoxic response curves of NLOC-015A against the cell lines. The growth percentage value of +100 on the Y-axis represents the growth of untreated cells, the 0 value represents no net growth, while -100 represents the complete death of cells.

Table 2. NCI synthetic compounds and investigational drugs sharing similar anti-cancer and mechanistic fingerprints with NLOC-015A

P	CCLC	Target NSC	NCI_Synthetic_Small Molecules	MW (g/mol)	NCI_Investigational and Mechanistic Drugs				
					P	CCLC	NSC	Target	
0.92	57	765599	NLOC-10B	350.334	0.75	59	778746	FH535	EGR-1/vegfr
0.88	59	765689	NLOC-21A	378.334	0.54	57	772886	Apatinib	VEGFR
0.76	59	50686	N-(4-chloro-2-methylphenyl)-3-hydroxynaphthalene-2-carboxamide	311.8	0.49	59	784590	Altiratinib	c-MET/TIE-2/VEGFR
0.73	57	765598	NLOC-2B	361.294	0.45	57	804518	Rogaratinib	Pan- FGFR
0.72	59	81947	5-bromo-N-(4-bromophenyl)-2-hydroxybenzamide	371.08	0.45	54	789968	LY3023414	PI3K/AKT
0.72	59	81947	Dibromsalan (USAN)	371.02	0.45	59	795718	BLU554	FGFR4
0.72	59	758440	Niclosamide (USAN)	327.12	0.45	57	751249	Dactolisib	PI3K
0.72	58	50683	N-(3-chlorophenyl)-3-hydroxynaphthalene-2-carboxamide	297.7	0.44	59	803248	MTX211	EGFR/P13K
0.71	59	756620	N-[3-[3,5-bis(trifluoromethyl)phenyl]c-[1,2,4]triazolo[3,4-b][1,3,4]thiadiazol-6-yl]cyclopentanecarboxamide	449.4	0.37	58	802451	CT-LY320	TGF-β
0.71	57	48444	4-chloro-2,6-bis[[5-chloro-3-(chloromethyl)-2-hydroxyphenyl]methyl]phenol	506.6	0.36	58	808507	CT-JNJ646	EGFR, MET
0.7	51	709566	N-(2-fluorophenyl)-7-hydroxy-2-[3-(trifluoromethyl)phenyl]iminochromene-3-carboxamide	442.2	0.36	59	754353	BKM-120 (PI3K)	P13K
0.68	47	709571	N-(4-fluorophenyl)-2-(3-fluorophenyl)imino-7-hydroxy-chromene-3-carboxamide	392.4	0.35	59	802820	FT1518	MTOR
0.68	58	791026	2-[(Z)-2-carboxy-1-(6-nitro-1H-benzimidazol-2-yl)ethenyl]-4-chlorophenolate	358.71	0.34	59	803248	MTX211	EGFR PI3K
0.67	57	179496	5,6-dichloro-2-hexyl-1H-imidazo[4,5-b]pyrazine	273.16	0.34	59	764515	Torkinib (PP242)	MTOR

Pearson's correlation coefficient. CCLC: Common cell lines count. MW: molecular weight. Seed Descriptor: S 765690.

A

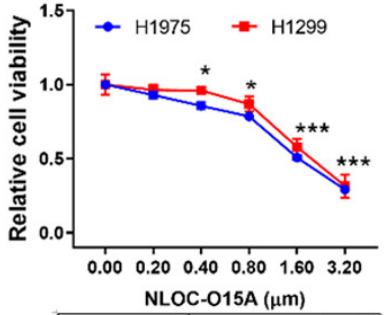

NSCLC_Cell	NLOC_015A (IC_{50})
H1299	1.90±0.23 μM
H1975	2.07±0.19 μM

B

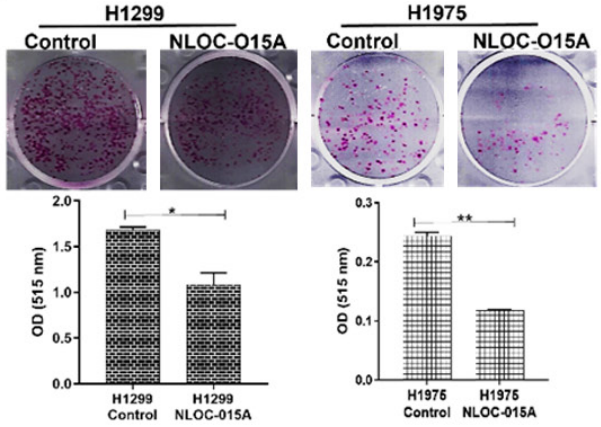

D

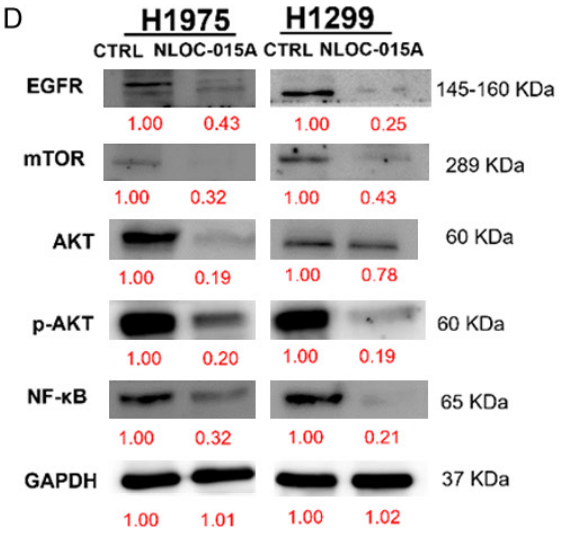

C

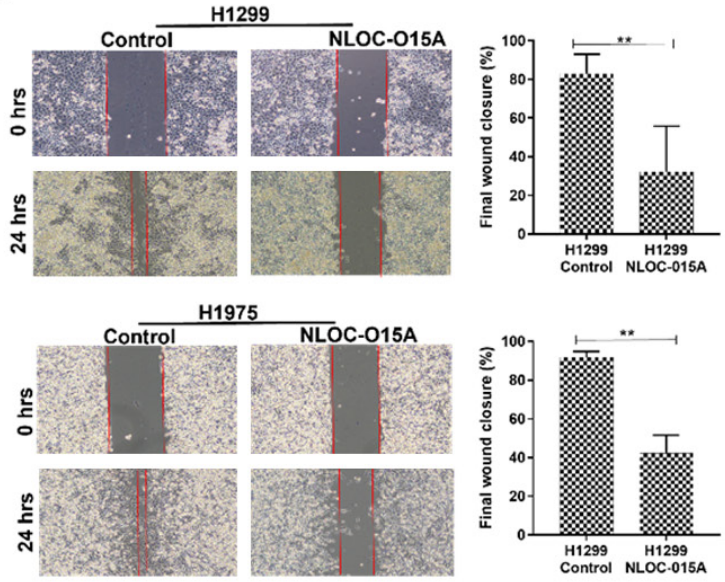

E

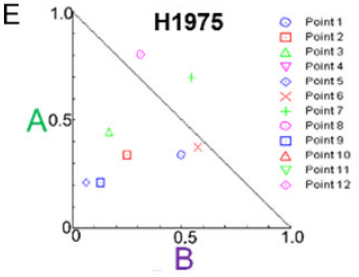

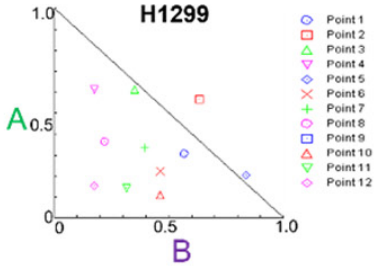

OSM (μM)	NLOC-015A (μM)	Effect	CI
4.0	1.6	0.66	0.83891
4.0	0.8	0.66	0.58823
4.0	0.4	0.56	0.61616
4.0	0.2	0.25	1.31441
2.0	0.16	0.58	0.27562
2.0	0.8	0.37	0.95180
2.0	0.4	0.19	1.24135
2.0	0.2	0.16	1.11611
1.0	0.16	0.33	0.34187
1.0	0.8	0.06	3.52397
1.0	0.4	0.04	2.91992
1.0	0.2	0.016	3.82891

OSM (μM)	NLOC-015A (μM)	Effect	CI
4.0	1.6	0.37	0.87608
4.0	0.8	0.29	1.19978
4.0	0.4	0.28	0.96748
4.0	0.2	0.28	0.79071
2.0	1.6	0.33	1.04558
2.0	0.8	0.32	0.68686
2.0	0.4	0.27	0.72891
2.0	0.2	0.26	0.58524
1.0	1.6	0.3	1.27138
1.0	0.8	0.32	0.57545
1.0	0.4	0.29	0.45855
1.0	0.2	0.28	0.33025

Figure 4. NL0C-015A compromised the cell viability and oncogenic phenotypes of non-small-cell lung cancer (NSCLC) via modulation of EGFR and PI3K-TOR signaling pathways. (A) NL0C-015A significantly suppressed the viability of H1299 and H1975 cells in dose-dependent manners. Graphical representation of the inhibitory effects of NL0C-015A on the (B) colony-forming, and (C) migratory abilities of H1299 and H1975 cells. (D) Western blot analysis showing that NL0C-015A suppressed expression levels of Akt, p-Akt, EGFR, mTOR, and NF-κB, in H1299 and H1975 cells compared to their vehicle-treated counterparts. (E) Representative right-angle isobologram triangles showing that NL0C-015A combined with osimertinib produced a synergetic effect. *P < 0.05, **P < 0.01, ***P < 0.001.

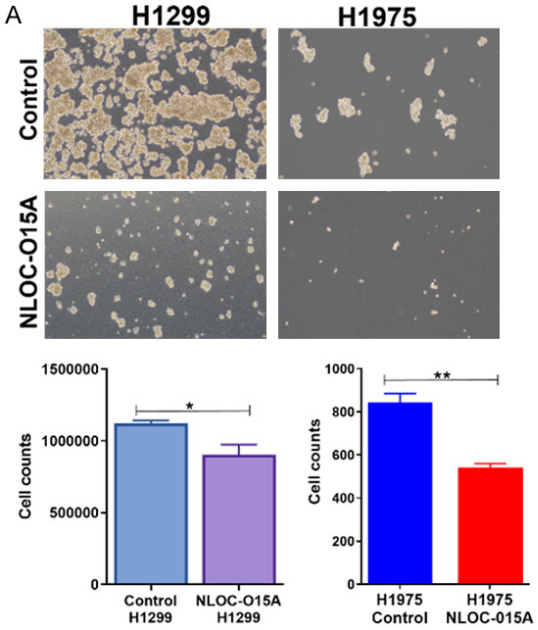

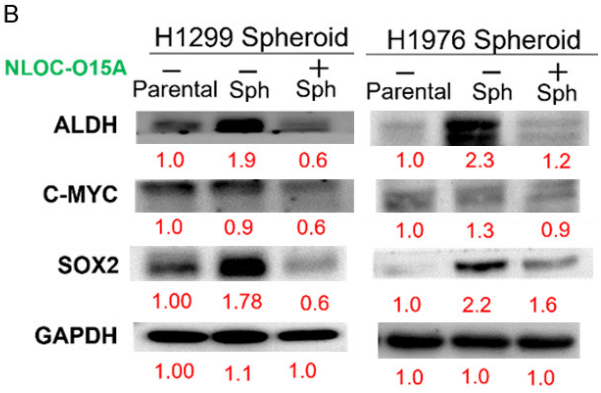

Figure 5. Effects of NL0C-015A treatment on the spheroid-forming abilities of H1299 and H1975 cells. Graphical representation of the inhibitory effects of NL0C-015A on the (A) spheroid-forming abilities of H1299 and H1975 cells. Scale bar 50 μm. (B) Western blot analysis showing that NL0C-015A suppressed expression levels of ALDH, c-Myc, and SOX2 in both H1299 and H1975 spheroid. *P < 0.05, **P < 0.01.

mice were attenuated by combined treatment (**Figure 7**).

Discussion

Lung cancer poses a serious threat to human health and has recently been tagged the second most common malignant disease with the highest incidence and mortality rate [1]. Despite the therapeutic advancement with chemotherapy and targeted therapy, the majority of NSCLC patients ultimately develop resistance to these drugs [3, 16]. There is, therefore, a need for the development of novel multitargeted therapies that can offer a high efficacy with lesser chances of drug resistance against NSCLC [66]. In the present study, we provide preclinical evidence of the therapeutic efficacy of NLOC-015A a multitarget small-molecule inhibitor of EGFR/mTOR/NF-Kb for the treatment NSCLC (**Figure 8**).

We demonstrated that NLOC-015A inhibited the proliferation and oncogenic attributes (colony formation, migration, and sphere formation) of H1975 and H1299 cells with concomitant downregulation of expression levels of oncogenic targets, including mTOR, Akt, NF-κB, EGFR, ALDH, c-Myc, and SOX2. Accumulating evidence indicates that combinations of two drugs in appropriate proportions often leads to higher therapeutic satisfaction and less chances of drug resistance compared to individual therapies [67, 68]. Interestingly, NLOC-015A synergized and enhanced the efficacy of osimertinib against NSCLC, providing a more cell viability inhibition compared to individual treatment. These data therefore suggested that NLOC-015 could be used to enhance the efficacy of osimertinib and possibly provide a solution to the recent emergence of osimertinib-resistance NSCLC.

In line with our in vitro data, NLOC-015A also demonstrated *in vivo* anticancer activities against an H1975-bearing xenograft mouse model. NLOC-015A inhibited proliferation, decreased the tumor burden, and enhanced the survival of mice compared to the control counterparts. In addition, NLOC-015A improved

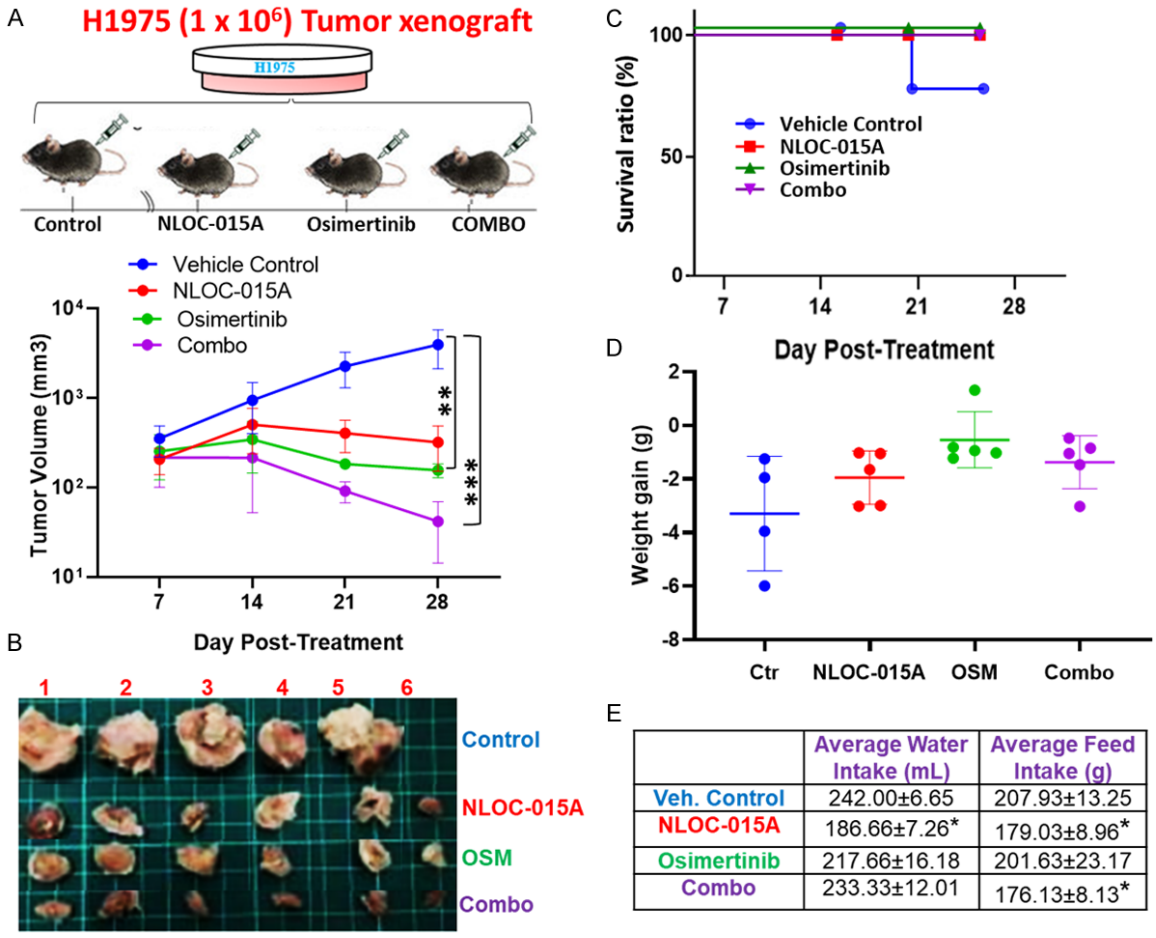

	Average Water Intake (mL)	Average Feed Intake (g)
Veh. Control	242.00±6.65	207.93±13.25
NLOC-015A	186.66±7.26*	179.03±8.96*
Osimertinib	217.66±16.18	201.63±23.17
Combo	233.33±12.01	176.13±8.13*

Figure 6. NLOC-015A suppressed tumorigenesis and enhanced the in vivo efficacy of osimertinib in a xenograft model of non-small-cell lung cancer (NSCLC). (A) Tumor burden vs. time curve, and (B) post-treatment tumor image showing the suppressive effect of NLOC-015A on H1975 xenograft-bearing mice. (C) Kaplan-Meier plot of survival, (D) body weight of treated mice, and (E) average feed/water intake compared to those in the control group. *P < 0.05, **P < 0.01, ***P < 0.001.

the BW gain of mice, suggesting the safety and absence of adverse effects of the compound when administered to mice. NLOC-015A also demonstrated a higher suppressive effect on tumor growth when combined with osimertinib. It was reported that inhibitors of mTOR and STAT3 appear to be the main mechanism of the enhanced antitumor efficacy of combination therapy in various cancers [68, 69].

Results of the present study also corroborate our previous findings, which indicated that the combination of a clinical drug with a small-molecule inhibitor of mTOR/CDK6/STAT3 offers a higher therapeutic index in in vitro and in vivo models of glioblastomas [39]. Altogether, our findings suggested that combining osimertinib with NLOC-015 appears to be a promising way to improve osimertinib's efficacy and achieve better therapeutic results against NSCLC. We therefore, suggest that NLOC-015A might represent a new candidate for treating NSCLC via acting as a multitarget inhibitor of EGFR/mTOR/NF-Kb signaling networks and efficiently compromising the oncogenic phenotype of NSCLC.

Liver and kidney impairment are common comorbidity for cancer patients either because of the disease itself, toxicity of anticancer treatments, or other factors affecting organ function [70]. Therefore, analysis of serum biochemical indices of liver and kidney function including ALT, AST, ALP, total proteins, creatinine, urea, and electrolytes concentrations are essential parameters in assessing the therapeutic outcome of anticancer agents. Consequently, we evaluated the effect of NLOC-015A treatment on hematological parameters and serum bio-

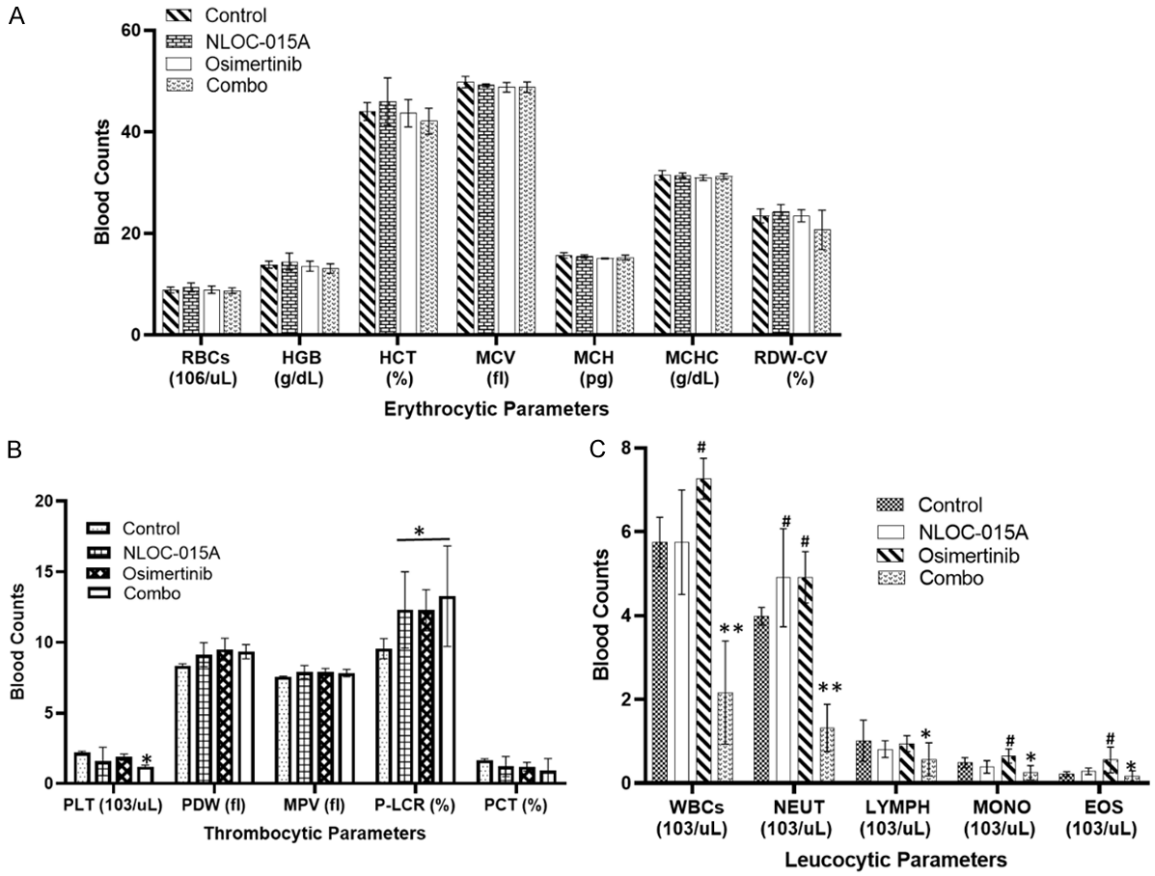

Figure 7. Effect of NLOC-015A treatment on hematological parameters of NSCLC tumor bearing mice. Bar graph of the effect of NLOC-015A treatment on (A) erythrocytic parameters, (B) thrombocytic parameters, and (C) leucocytic parameters in NSCLC tumor bearing mice. *P < 0.01, **P < 0.01, ***P < 0.001. # significant high expression compared to the control group.

Table 3. Effect of NLOC-015A treatment on hematological parameters of NSCLC tumor bearing mice

	Vehicle	NLOC-015A	Osimertinib	Combo
SGPT (U/l)	351.00±130.51[b]	86.00±2.94[a]	88.50±6.65[a]	80.00±6.68[a]
SGOT (U/l)	927.00±236.96[b]	497.00±88.50[a,b]	440.50±251.59[a,b]	168.00±70.29[a]
TP (g/dl)	5.90±0.35[b]	5.85±0.10[b]	6.10±0.17[b]	2.89±1.00[a]
TBIL (mg/dl)	2.20±0.38[a]	1.60±0.34[a]	1.70±0.90[a]	1.20±0.08[a]
CRE (mg/dl)	0.47±0.01[a]	0.46±0.03[a]	0.61±0.07[b]	0.44±0.11[a]
UA (mg/dl)	4.20±0.70[b]	2.55±0.19[a,b]	1.80±0.92[a]	1.65±0.38[a]
Na (mEq/ml)	127.10±37.25[a]	165.50±4.57[a]	163.50±2.63[a]	182.00±9.35[a]
K (mEq/ml)	126.85±60.82[a,b,c]	202.80±31.13[b,c]	280.40±70.40[c]	21.05±16.73[a]
Cl (mEq/ml)	125.50±4.65[a]	119.50±1.89[a]	123.00±2.52[a]	150.00±4.55[b]

Values with different superscript alphabet (a, b, c) are significantly different (p<0.05).

chemical markers of hepatic and kidney function in the NSCLC tumor-bearing mice. The elevated levels of the AST, ALT, total proteins, and uric acid (UA) in NSCLC tumor-bearing mice suggested that the integrity of the liver and kidney has been compromised. In line with our findings, Cao et al. [71], reported elevated levels of ALT, AST and AKP in cancer patients [71]. Interestingly, the reversal effects of NLOC-015A on the serum biochemical indices suggested its safety profile as well as its attenuative effects on hepatorenal impairment in NSCLC bearing mice. Toxicity of osimertinib has been documented [72]. Our analysis revealed that

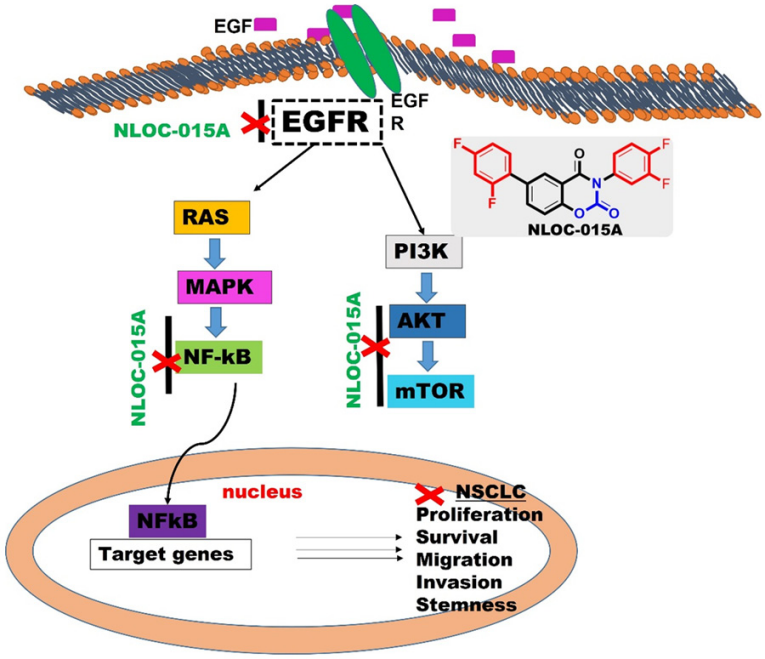

Figure 8. Schematic representation of the mechanism of action of NLOC-015. NLOC-015 compromised the proliferation, stemness and oncogenic phenotypes of NSCLC via multi target inhibition of EGFR-AKT/mTOR/NF-kB signaling networks.

the combination of NLOC-015A with osimertinib reversed the elevation in potassium and creatinine levels that were observed in osimertinib-treated mice.

The hematopoietic system is a crucial component of the body system that regulates various physiological and pathological conditions [73]. Hematological parameters including PCV, HB, WBC, RBC PLT are important component of hematopoietic system that plays a pivotal role in the body defense and disease conditions and are well known to be susceptible to obliteration by toxicant, foreign substances, therapeutic agents, and diseases conditions including cancers [74-77]. Our analysis of hematological parameters identified leukocytosis, characterized by elevated WBCs, neutrophils (NEUTs), monocytes (MONOs), and eosinophils (EOSs), in osimertinib-treated mice. However, combined treatment with osimertinib and NLOC-015A significantly ameliorated the elevated leucocytic indices. Collectively, these findings suggested that NLOC-015A, not only enhanced the efficacy of osimertinib but also alleviated its toxic effects, thus may serve as attractive strategies for the treatment of NSCLC. However, the limitation of our study must be acknowledged. The absence of pharmacokinetic studies to ascertain the drug likeness of the compound marked a critical area that required further studies. Therefore, studies are currently ongoing to elucidate the in vivo pharmacokinetics and drug distribution of NLOC-015A in in vivo animal model.

Conclusions

In conclusion, we provide preclinical evidence of the therapeutic efficacy of NLOC-015A a multitarget small-molecule inhibitor of epidermal growth factor receptor (EGFR)/mammalian target of rapamycin (mTOR)/AKT, nuclear factor (NF)-κB for the treatment NSCLC. Our findings suggested that combining osimertinib with NLOC-015A appears to be a promising way to improve osimertinib's efficacy and achieve better therapeutic results against NSCLC. NLOC-015A, not only enhanced the efficacy of osimertininb but also attenuated its toxicity. We therefore suggest that NLOC-015A might represent a new candidate for treating NSCLC. Further pre-clinical study to evaluate the full therapeutic properties of NLOC-015A for the treatment of NSCLC is ongoing in our laboratory.

Acknowledgements

The National Science and Technology Council, Taiwan, grant number NSTC111-2314-B-038-017, the Ministry of Science and Technology, Taiwan, grant number MOST111-2314-B-038-122, and the Shin Kong Wu Ho-Su Memorial Hospital SKH-TMU-112-02 awarded to H.-S. Huang. ATH Wu is funded by The National Science and Technology Council, Taiwan, grant numbers 111-2314-B-038-098 and 111-2314-B-038-142.

Disclosure of conflict of interest

The authors declare that the research was conducted in the absence of any commercial or

financial relationships that could be construed as a potential conflict of interest.

Address correspondence to: Alexander TH Wu, The PhD Program of Translational Medicine, College of Medical Science and Technology, Taipei Medical University, Taipei 11031, Taiwan. E-mail: chaw1211@tmu.edu.tw; Hsu-Shan Huang, Graduate Institute of Medical Sciences, National Defense Medical Center, Taipei 11490, Taiwan. E-mail: huanghs99@tmu.edu.tw

References

[1] Sung H, Ferlay J, Siegel RL, Laversanne M, Soerjomataram I, Jemal A and Bray F. Global cancer statistics 2020: GLOBOCAN estimates of incidence and mortality worldwide for 36 cancers in 185 countries. CA Cancer J Clin 2021; 71: 209-249.

[2] Osmani L, Askin F, Gabrielson E and Li QK. Current WHO guidelines and the critical role of immunohistochemical markers in the subclassification of non-small cell lung carcinoma (NSCLC): moving from targeted therapy to immunotherapy. Semin Cancer Biol 2018; 52: 103-109.

[3] Tian X, Gu T, Lee MH and Dong Z. Challenge and countermeasures for EGFR targeted therapy in non-small cell lung cancer. Biochim Biophys Acta Rev Cancer 2022; 1877: 188645.

[4] Jemal A, Bray F, Center MM, Ferlay J, Ward E and Forman D. Global cancer statistics. CA Cancer J Clin 2011; 61: 69-90.

[5] Tan Q, Lin S, Zeng Y, Yao M, Liu K, Yuan H, Liu C and Jiang G. Ginsenoside Rg3 attenuates the osimertinib resistance by reducing the stemness of non-small cell lung cancer cells. Environ Toxicol 2020; 35: 643-651.

[6] Mu Y, Hao X, Yang K, Ma D, Wang S, Xu Z, Li J and Xing P. Clinical modality of resistance and subsequent management of patients with advanced non-small cell lung cancer failing treatment with osimertinib. Target Oncol 2019; 14: 335-342.

[7] Malhotra J, Malvezzi M, Negri E, La Vecchia C and Boffetta P. Risk factors for lung cancer worldwide. Eur Respir J 2016; 48: 889-902.

[8] Ma Z, Zhang Y, Deng C, Fu F, Deng L, Li Y and Chen H. The prognostic value of Kirsten rat sarcoma viral oncogene homolog mutations in resected lung adenocarcinoma differs according to clinical features. J Thorac Cardiovasc Surg 2022; 163: e73-e85.

[9] Metro G and Crinò L. Advances on EGFR mutation for lung cancer. Transl Lung Cancer Res 2012; 1: 5-13.

[10] Califano R, Morgillo F, De Mello RA and Mountzios G. Role of mesenchymal-epithelial transition amplification in resistance to anti-epidermal growth factor receptor agents. Ann Transl Med 2015; 3: 81.

[11] Ritter CA and Arteaga CL. The epidermal growth factor receptor-tyrosine kinase: a promising therapeutic target in solid tumors. Semin Oncol 2003; 30 Suppl 1: 3-11.

[12] Lazzara MJ, Lane K, Chan R, Jasper PJ, Yaffe MB, Sorger PK, Jacks T, Neel BG and Lauffenburger DA. Impaired SHP2-mediated extracellular signal-regulated kinase activation contributes to gefitinib sensitivity of lung cancer cells with epidermal growth factor receptor-activating mutations. Cancer Res 2010; 70: 3843-3850.

[13] Karachaliou N, Fernandez-Bruno M, Bracht JWP and Rosell R. EGFR first- and second-generation TKIs-there is still place for them in EGFR-mutant NSCLC patients. Transl Cancer Res 2019; 8 Suppl 1: S23-S47.

[14] Scaltriti M and Baselga J. The epidermal growth factor receptor pathway: a model for targeted therapy. Clin Cancer Res 2006; 12: 5268-5272.

[15] Wu SG and Shih JY. Management of acquired resistance to EGFR TKI-targeted therapy in advanced non-small cell lung cancer. Mol Cancer 2018; 17: 38.

[16] Higgins KA, Puri S and Gray JE. Systemic and radiation therapy approaches for locally advanced non-small-cell lung cancer. J Clin Oncol 2022; 40: 576-585.

[17] Zhong L, Li Y, Xiong L, Wang W, Wu M, Yuan T, Yang W, Tian C, Miao Z, Wang T and Yang S. Small molecules in targeted cancer therapy: advances, challenges, and future perspectives. Signal Transduct Target Ther 2021; 6: 201.

[18] Petrelli A and Valabrega G. Multitarget drugs: the present and the future of cancer therapy. Expert Opin Pharmacother 2009; 10: 589-600.

[19] Lawal B, Kuo YC, Tang SL, Liu FC, Wu ATH, Lin HY and Huang HS. Transcriptomic-based identification of the immuno-oncogenic signature of cholangiocarcinoma for HLC-018 multi-target therapy exploration. Cells 2021; 10: 2873.

[20] Huang HS, Chiu HF, Lee AL, Guo CL and Yuan CL. Synthesis and structure-activity correlations of the cytotoxic bifunctional 1,4-diamidoanthraquinone derivatives. Bioorg Med Chem 2004; 12: 6163-6170.

[21] Huang HS, Chiu HF, Yeh PF and Yuan CL. Structure-based design and synthesis of regioisomeric disubstituted aminoanthraquinone derivatives as potential anticancer agents. Helv Chim Acta 2004; 87: 999-1006.

[22] Huang HS, Yu DS and Chen TC. Novel thiochromeno[2,3-c]quinolin-12-one derivatives, preparation method and application thereof. Google Patent 2015.
[23] Khedkar HN, Wang YC, Yadav VK, Srivastava P, Lawal B, Mokgautsi N, Sumitra MR, Wu ATH and Huang HS. In-silico evaluation of genetic alterations in ovarian carcinoma and therapeutic efficacy of NSC777201, as a novel multi-target agent for TTK, NEK2 and CDK1. Int J Mol Sci 2021; 22: 5895.
[24] Lawal B, Kuo YC, Sumitra MR, Wu ATH and Huang HS. In vivo pharmacokinetic and anticancer studies of HH-N25, a selective inhibitor of topoisomerase I, and hormonal signaling for treating breast cancer. J Inflamm Res 2021; 14: 4901-4913.
[25] Lawal B, Kuo YC, Wu ATH and Huang HS. BC-N102 suppress breast cancer tumorigenesis by interfering with cell cycle regulatory proteins and hormonal signaling, and induction of time-course arrest of cell cycle at G1/G0 phase. Int J Biol Sci 2021; 17: 3224-3238.
[26] Lawal B, Lee CY, Mokgautsi N, Sumitra MR, Khedkar H, Wu ATH and Huang HS. mTOR/EGFR/iNOS/MAP2K1/FGFR/TGFB1 are druggable Candidates for N-(2,4-difluorophenyl)-2',4'-difluoro-4-hydroxybiphenyl-3-carboxamide (NSC765598), with consequent anticancer implications. Front Oncol 2021; 11: 656738.
[27] Lawal B, Liu YL, Mokgautsi N, Khedkar H, Sumitra MR, Wu ATH and Huang HS. Pharmacoinformatics and preclinical studies of NSC76-5690 and NSC765599, potential STAT3/CDK2/4/6 inhibitors with antitumor activities against NCI60 human tumor cell lines. Biomedicines 2021; 9: 92.
[28] Lawal B, Wang YC, Wu ATH and Huang HS. Prooncogenic c-Met/EGFR, biomarker signatures of the tumor microenvironment are clinical and therapy response prognosticators in colorectal cancer, and therapeutic targets of 3-Phenyl-2H-benzo[e][1,3]-Oxazine-2,4(3H)-Dione derivatives. Front Pharmacol 2021; 12: 691234.
[29] Lee CC, Huang KF, Chang DM, Hsu JJ, Huang FC, Shih KN, Chen CL, Chen TC, Chen RH, Lin JJ and Huang HS. Design, synthesis and evaluation of telomerase inhibitory, hTERT repressing, and anti-proliferation activities of symmetrical 1,8-disubstituted amidoanthraquinones. Eur J Med Chem 2012; 50: 102-112.
[30] Lee CC, Liu FL, Chen CL, Chen TC, Chang DM and Huang HS. Discovery of 5-(2',4'-difluorophenyl)-salicylanilides as new inhibitors of receptor activator of NF-κB ligand (RANKL)-induced osteoclastogenesis. Eur J Med Chem 2015; 98: 115-126.
[31] Lee CC, Liu FL, Chen CL, Chen TC, Liu FC, Ahmed Ali AA, Chang DM and Huang HS. No0 vel inhibitors of RANKL-induced osteoclastogenesis: design, synthesis, and biological evaluation of 6-(2,4-difluorophenyl)-3-phenyl-2H-benzo[e][1,3]oxazine-2,4(3H)-diones. Bioorg Med Chem 2015; 23: 4522-4532.
[32] Lee JC, Wu ATH, Chen JH, Huang WY, Lawal B, Mokgautsi N, Huang HS and Ho CL. HNC0014, a multi-targeted small-molecule, inhibits head and neck squamous cell carcinoma by suppressing c-Met/STAT3/CD44/PD-L1 oncoimmune signature and eliciting antitumor immune responses. Cancers (Basel) 2020; 12: 3759.
[33] Liu FC, Lu JW, Chien CY, Huang HS, Lee CC, Lien SB, Lin LC, Chen LW, Ho YJ, Shen MC, Ho LJ and Lai JH. Arthroprotective effects of Cf-02 sharing structural similarity with quercetin. Int J Mol Sci 2018; 19: 1453.
[34] Madamsetty VS, Pal K, Dutta SK, Wang E, Thompson JR, Banerjee RK, Caulfield TR, Mody K, Yen Y, Mukhopadhyay D and Huang HS. Design and evaluation of PEGylated liposomal formulation of a novel multikinase inhibitor for enhanced chemosensitivity and inhibition of metastatic pancreatic ductal adenocarcinoma. Bioconjug Chem 2019; 30: 2703-2713.
[35] Mokgautsi N, Wang YC, Lawal B, Khedkar H, Sumitra MR, Wu AT and Huang HS. Network pharmacological analysis through a bioinformatics approach of novel NSC765600 and NSC765691 compounds as potential inhibitors of CCND1/CDK4/PLK1/CD44 in cancer types. Cancers (Basel) 2021; 13: 2523.
[36] Mokgautsi N, Wen YT, Lawal B, Khedkar H, Sumitra MR, Wu AT and Huang HS. An integrated bioinformatics study of a novel niclosamide derivative, nsc765689, a potential gsk3β/β-catenin/stat3/cd44 suppressor with anti-glioblastoma properties. Int J Mol Sci 2021; 22: 2464.
[37] Shen CJ, Lin PL, Lin HC, Cheng YW, Huang HS and Lee H. RV-59 suppresses cytoplasmic Nrf2-mediated 5-fluorouracil resistance and tumor growth in colorectal cancer. Am J Cancer Res 2019; 9: 2789-2796.
[38] Yadav VK, Huang YJ, George TA, Wei PL, Sumitra MR, Ho CL, Chang TH, Wu ATH and Huang HS. Preclinical evaluation of the novel small-molecule MSI-N1014 for treating drug-resistant colon cancer via the LGR5/β-catenin/miR-142-3p network and reducing cancer-associated fibroblast transformation. Cancers (Basel) 2020; 12: 1590.
[39] Wu ATH, Huang HS, Wen YT, Lawal B, Mokgautsi N, Huynh TT, Hsiao M and Wei L. A preclinical investigation of GBM-N019 as a potential inhibitor of glioblastoma via exosomal mTOR/CDK6/STAT3 signaling. Cells 2021; 10: 2391.
[40] SAMPLES IB. Serial review: flavonoids and isoflavones (photoestrogens): absorption, metab-

olism and bioactivity. Free Rad Biol Med 2004; 37: 1324-1350.
[41] Erlund I. Review of the flavonoids quercetin, hesperetin and naringenin. Dietary sources, bioactivities, bioavailability and epidemiology. Nutr Res 2004; 24: 851-874.
[42] Snetkov P, Morozkina S, Olekhnovich R and Uspenskaya M. Diflunisal targeted delivery systems: a review. Materials (Basel) 2021; 14: 6687.
[43] Li Y, Li PK, Roberts MJ, Arend RC, Samant RS and Buchsbaum DJ. Multi-targeted therapy of cancer by niclosamide: a new application for an old drug. Cancer Lett 2014; 349: 8-14.
[44] Kadri H, Lambourne OA and Mehellou Y. Niclosamide, a drug with many (re)purposes. ChemMedChem 2018; 13: 1088-1091.
[45] Jasial S, Hu Y and Bajorath J. Assessing the growth of bioactive compounds and scaffolds over time: implications for lead discovery and scaffold hopping. J Chem Inf Model 2016; 56: 300-307.
[46] Vichai V and Kirtikara K. Sulforhodamine B colorimetric assay for cytotoxicity screening. Nat Protoc 2006; 1: 1112-1116.
[47] Chou TC. Drug combination studies and their synergy quantification using the Chou-Talalay method. Cancer Res 2010; 70: 440-446.
[48] Chou TC and Talalay P. Quantitative analysis of dose-effect relationships: the combined effects of multiple drugs or enzyme inhibitors. Adv Enzyme Regul 1984; 22: 27-55.
[49] Franken NA, Rodermond HM, Stap J, Haveman J and van Bree C. Clonogenic assay of cells in vitro. Nat Protoc 2006; 1: 2315-2319.
[50] Ma HP, Chang HL, Bamodu OA, Yadav VK, Huang TY, Wu ATH, Yeh CT, Tsai SH and Lee WH. Collagen 1A1 (COL1A1) is a reliable biomarker and putative therapeutic target for hepatocellular carcinogenesis and metastasis. Cancers (Basel) 2019; 11: 786.
[51] Mahmood T and Yang PC. Western blot: technique, theory and trouble shooting. N Am J Med Sci 2012; 4: 429-434.
[52] Wu ATH, Srivastava P, Yadav VK, Tzeng DTW, Iamsaard S, Su EC, Hsiao M and Liu MC. Ovatodiolide, isolated from anisomeles indica, suppresses bladder carcinogenesis through suppression of mTOR/β-catenin/CDK6 and exosomal miR-21 derived from M2 tumor-associated macrophages. Toxicol Appl Pharmacol 2020; 401: 115109.
[53] Lawal B, Wu AT, Chen CH, T A G and Wu SY. Identification of INFG/STAT1/NOTCH3 as γ-Mangostin's potential targets for overcoming doxorubicin resistance and reducing cancer-associated fibroblasts in triple-negative breast cancer. Biomed Pharmacother 2023; 163: 114800.
[54] Olugbodi JO, David O, Oketa EN, Lawal B, Okoli BJ and Mtunzi F. Silver nanoparticles stimulates spermatogenesis impairments and hematological alterations in testis and epididymis of male rats. Molecules 2020; 25: 1063.
[55] Lawal B, Shittu OK, Oibiokpa FI, Mohammed H, Umar SI and Haruna GM. Antimicrobial evaluation, acute and sub-acute toxicity studies of allium sativum. J Acute Dis 2016; 5: 296-301.
[56] Dacie J and Lewis S. Practical textbook of haematology 7th edition edinburgh. Church Livingstone 1991; 7: 54-79.
[57] De Ritis F, Coltorti M and Giusti G. Serum-transaminase activities in liver disease. Lancet 1972; 1: 685-687.
[58] Rej R. Measurement of aminotransferases: part 1. Aspartate aminotransferase. Crit Rev Clin Lab Sci 1984; 21: 99-186.
[59] Gornall AG, Bardawill CJ and David MM. Determination of serum proteins by means of the biuret reaction. J Biol Chem 1949; 177: 751-766.
[60] Suzuki Y and Sakagishi Y. Determination of serum bilirubin by the diazo method using the diazotized 3-Nitroaniline reacting readily with the photoproducts of bilirubin. Clinical Chemistry 1994; 23: 158-163.
[61] Doumas BT, Watson WA and Biggs HG. Albumin ST andards and the measurement of serum albumin with bromcresol green. Clin Chim Acta 1971; 31: 87-96.
[62] Delanghe JR and Speeckaert MM. Creatinine determination according to Jaffe-what does it stand for? NDT Plus 2011; 4: 83-86.
[63] Searle PL. The berthelot or indophenol reaction and its use in the analytical chemistry of nitrogen. A review. Analyst 1984; 109: 549-568.
[64] Alley MC, Scudiero DA, Monks A, Hursey ML, Czerwinski MJ, Fine DL, Abbott BJ, Mayo JG, Shoemaker RH and Boyd MR. Feasibility of drug screening with panels of human tumor cell lines using a microculture tetrazolium assay. Cancer Res 1988; 48: 589-601.
[65] Shoemaker RH. The NCI60 human tumour cell line anticancer drug screen. Nat Rev Cancer 2006; 6: 813-823.
[66] Yumura M, Nagano T and Nishimura Y. Novel multitarget therapies for lung cancer and respiratory disease. Molecules 2020; 25: 3987.
[67] Taylor JW, Parikh M, Phillips JJ, James CD, Molinaro AM, Butowski NA, Clarke JL, Oberheim-Bush NA, Chang SM, Berger MS and Prados M. Phase-2 trial of palbociclib in adult patients with recurrent RB1-positive glioblastoma. J Neurooncol 2018; 140: 477-483.
[68] Franco J, Balaji U, Freinkman E, Witkiewicz AK and Knudsen ES. Metabolic reprogramming of pancreatic cancer mediated by CDK4/6 inhibi-

tion elicits unique vulnerabilities. Cell Rep 2016; 14: 979-990.
[69] Kettner NM, Vijayaraghavan S, Durak MG, Bui T, Kohansal M, Ha MJ, Liu B, Rao X, Wang J, Yi M, Carey JPW, Chen X, Eckols TK, Raghavendra AS, Ibrahim NK, Karuturi MS, Watowich SS, Sahin A, Tweardy DJ, Hunt KK, Tripathy D and Keyomarsi K. Combined inhibition of STAT3 and DNA repair in palbociclib-resistant ER-positive breast cancer. Clin Cancer Res 2019; 25: 3996-4013.
[70] Krens SD, Lassche G, Jansman FGA, Desar IME, Lankheet NAG, Burger DM, van Herpen CML and van Erp NP. Dose recommendations for anticancer drugs in patients with renal or hepatic impairment. Lancet Oncol 2019; 20: e200-e207.
[71] Cao WX, Cheng QM, Fei XF, Li SF, Yin HR and Lin YZ. A study of preoperative methionine-depleting parenteral nutrition plus chemotherapy in gastric cancer patients. World J Gastroenterol 2000; 6: 255-258.
[72] Anand K, Ensor J, Trachtenberg B and Bernicker EH. Osimertinib-induced cardiotoxicity: a retrospective review of the FDA adverse events reporting system (FAERS). JACC CardioOncol 2019; 1: 172-178.
[73] Shittu OK, Lawal B, Alozieuwa BU, Haruna GM, Abubakar AN and Berinyuy EB. Alteration in biochemical indices following chronic administration of methanolic extract of nigeria bee propolis in Wistar rats. Asian Pac J Trop Dis 2015; 5: 654-657.
[74] Mukthavaram R, Shi G, Kesari S and Simberg D. Targeting and depletion of circulating leukocytes and cancer cells by lipophilic antibody-modified erythrocytes. J Control Release 2014; 183: 146-153.
[75] Bashir L, Shittu O, Busari M, Sani S and Aisha M. Safety evaluation of giant African l and snails (archachatina maginata) haemolymph on hematological and biochemical parameters of albino rats. J Adv Med Pharm Sci 2015; 122-130.
[76] Berinyuy EB, Lawal B, Olalekan AA, Olalekan IA, Yusuf AA, Sakpe S and Ossai PC. Hematological status and organs/body-weight parameters in Wister rats during chronic administration of cassia occidentalis. Int Blood Res Rev 2015; 4: 1-7.
[77] Atzil S, Arad M, Glasner A, Abiri N, Avraham R, Greenfeld K, Rosenne E, Beilin B and Ben-Eliyahu S. Blood transfusion promotes cancer progression: a critical role for aged erythrocytes. Anesthesiology 2008; 109: 989-997.

Table S1. *In silico* structural-activity relationship profile of NLOC-015A based on PASS (prediction of activity spectra for substances) algorithm

Score	Activities
0.735	Biliary tract disorders treatment
0.602	Neurodegenerative diseases treatment
0.573	Antineurotic
0.426	Antineoplastic
0.344	Cyclooxygenase inhibitor
0.317	Hepatic and renal disorders treatment
0.331	Prostate disorders treatment
0.362	Antiinflammatory
0.230	Interleukin 10 agonist
0.148	Macrophage migration inhibitory factor inhibitor
0.096	Transcription factor STAT6 inhibitor
0.102	MAP-kinase-activated kinase 2 inhibitor
0.110	EGF expression inhibitor
0.110	MAP-kinase-activated kinase inhibitor
0.252	Phosphatidylcholine-retinol O-acyltransferase inhibitor

Table S2. Specific anti-cancer profiling of NLOC-015A against common cancer cell lines based on PASS (prediction of activity spectra for substances) algorithm

Pa	Pi	Cell-line	Full name	Tissue	Tumor type
0.424	0.083	A549	Lung carcinoma	Lung	Carcinoma
0.124	0.103	NCI-H128	Small cell lung cancer	Lung	Carcinoma
0.231	0.169	Hs-578T	Invasive ductal breast carcinoma	Breast	Carcinoma
0.270	0.092	CWR22R	Prostate carcinoma epithelial cell line	Prostate	Carcinoma
0.278	0.109	PC-3	Prostate carcinoma	Prostate	Carcinoma
0.289	0.078	HuP-T3	Pancreatic adenocarcinoma	Pancreas	Adenocarcinoma
0.296	0.188	CFPAC-1	Pancreatic carcinoma	Pancreas	Carcinoma
0.318	0.127	RKO	Colon carcinoma	Colon	Carcinoma
0.403	0.049	HCT-116	Colon carcinoma	Colon	Carcinoma
0.424	0.083	A549	Lung carcinoma	Lung	Carcinoma